SERI/TR-631-336 April 1980

Optical Analysis of Point Focus Parabolic Radiation Concentrators

Paul Bendt
Ari Rabl

SERI

Solar Energy Research Institute
A Division of Midwest Research Institute

1617 Cole Boulevard
Golden, Colorado 80401

Operated for the
U.S. Department of Energy
under Contract No. EG-77-C-01-4042

Printed in the United States of America
Available from:
National Technical Information Service
U.S. Department of Commerce
5285 Port Royal Road
Springfield, VA 22161
Price:
Microfiche $3.00
Printed Copy $4.50

NOTICE

SERI/TR-631-336
UC CATEGORY: UC-62

OPTICAL ANALYSIS OF POINT FOCUS PARABOLIC RADIATION CONCENTRATORS

PAUL BENDT
ARI RABL

APRIL 1980

PREPARED UNDER TASK NO. 3527

Solar Energy Research Institute

1536 Cole Boulevard
Golden, Colorado 80401

A Division of Midwest Research Institute

Prepared for the
U.S. Department of Energy
Contract No. EG-77-C-01-4042

FOREWORD

This report documents work done on Task 3527 in the Solar Thermal Research Branch of the Solar Energy Research Institute.

Frank Kreith

Frank Kreith, Branch Chief
Solar Thermal Research Branch

Approved for:

SOLAR ENERGY RESEARCH INSTITUTE

K. J. Touryan

K. J. Touryan, Acting Manager
Solar Thermal, Ocean, and Wind Division

SUMMARY

A simple formalism is developed for analyzing the optical performance of point focus parabolic radiation concentrators. To account for off-axis aberrations of the parabola, an angular acceptance function is defined as that fraction of a beam of parallel radiation incident on the aperture which would reach the receiver if the optics were perfect. The radiation intercepted by the receiver of a real concentrator is obtained as a convolution of angular acceptance function, of optical error distribution, and of angular brightness distribution of the radiation source. Losses resulting from absorption in the reflector or reflection at the receiver are treated by a multiplicative factor $\rho\alpha$ where ρ = reflectance of the reflector and α = absorptance of the receiver. For numerical calculations, this method is more accurate and less time-consuming than the ray-tracing method. In many cases, there are acceptable approximations whereby the results can be obtained by reading a graph or evaluating a simple curve fit.

TABLE OF CONTENTS

LIST OF FIGURES

LIST OF TABLES

NOMENCLATURE

a	=	ratio of absorber radius over focal length
b	=	ratio of reflector radius over focal length
$B_{source}(\vec{\theta})$	=	angular profile of source (W/m^2 sterad)
$B_{eff}(\vec{\theta})$	=	effective source (W/m^2 sterad)
	=	convolution of source profile $B_{source}(\vec{\theta})$ and distribution function $E(\vec{\theta})$ of optical errors
C	=	geometric concentration ratio
	=	ratio of aperture area over receiver surface area
$E_{optical}(\vec{\theta})$	=	distribution function of optical errors ($sterad^{-1}$)
$f(\theta)$	=	angular acceptance function
	=	fraction of rays incident on aperture at incidence angle θ from optical axis, which reach receiver
I_b	=	beam component of solar irradiance (W/m^2), as measured by pyrheliometer
I_{in}	=	that portion of I_b which reaches the receiver (in W per m^2 of aperture area)
α	=	absorptance of receiver
γ	=	intercept factor I_{in}/I_b
Φ	=	rim angle
$\sigma_{optical}$	=	angular spread caused by all optical errors
σ_{source}	=	angular width of source
σ	=	total beam spread
ρ	=	reflectance of reflector

SECTION 1.0

INTRODUCTION

Parabolic reflectors are employed to concentrate incoming radiation onto a smaller receiver. For example, in solar energy applications, concentrators can reduce heat losses in thermal collectors (Rabl 1976); and in radiation detectors, the signal-to-noise ratio may be improved if the incident radiation is concentrated onto a smaller receiver (Harper et al. 1976). In these situations, the incident rays come from a range of directions (e.g., from the entire solar disk) and their angular spread is further increased by optical errors. Optical errors may be caused by deviations of the reflector surface from the specified parabolic contour, by lack of perfect specularity of the reflector material (Pettit 1977; Butler and Pettit 1977), by displacement of the receiver from its design position, etc. In these applications, the imaging properties of the parabola are not directly relevant--one needs to know how much of the incident radiation is intercepted by the receiver and, perhaps, the spatial or angular intensity distribution, but the exact correspondence between points of the radiation source and impact points on the receiver is immaterial.

Traditionally, the optical analysis of radiation concentrators has been carried out by means of computer ray-trace programs* (Biggs and Vittoe; Schrenk 1963). Ray tracing is a microscopic method that can provide an enormous amount of numerical information but obscures functional relationships. Recognition of functional relationships is extremely useful for design optimization. Recently, an interesting analytical solution for the optical performance of parabolic dish reflectors with flat receivers was presented by O'Neill and Hudson (1978). Their method for calculating the optical performance is fast and accurate but assumes that the radiation source is a uniform disk. Many situations require greater flexibility because the source is not uniform. Examples are the effect of solar limb darkening (the edge of the solar disk is darker than the center), the effect of circumsolar radiation (Bendt and Rabl 1979), and the effect of misalignment between source and reflector (Bendt, Gaul, and Rabl 1979). In order to deal with these problems, we have developed a technique which is not only more flexible than that of O'Neill and Hudson (1978), but far more convenient to use.

The present paper shows how all the relevant parameters for the design of parabolic concentrators can be obtained by a simple macroscopic approach which takes advantage of the fact that imaging information is not needed. All quantities of interest are calculated analytically. In order to account for off-axis aberrations of the parabola, an <u>angular acceptance function</u> is defined as

*For a survey of the subject, see L. Wen et al., 1979.

that fraction of a parallel beam of radiation incident on the aperture which would reach the receiver if the optics were perfect. The radiation intercepted by the receiver of a real concentrator is obtained as a convolution of angular acceptance function, of optical error distribution, and of angular brightness distribution of the radiation source. Losses resulting from absorption in the reflector or reflection at the receiver are treated by a multiplicative factor $\rho\alpha$, where ρ = reflectance of the reflector and α = absorptance of the receiver. For numerical calculations, this method is more accurate and faster than ray tracing. In its present form, it is limited to parabolic reflectors. However, even for the study of arbitrary reflector shapes, the present method may serve as a useful tool for evaluating the accuracy of ray-trace programs.

This paper is organized as follows. In Section 2.0, the angular acceptance function of the parabolic dish reflector is calculated exactly, for both spherical and flat receivers, and a simple analytical curve fit that has sufficient accuracy for most applications is provided. In Section 3.0, the angular acceptance function is convoluted with optical errors and brightness distribution of the source. In Section 4.0, the usefulness of this method is illustrated for the case of an effective source of radiation with gaussian distribution; in this case, the result is obtained in closed form.

SECTION 2.0

ANGULAR ACCEPTANCE FUNCTION

The form of the angular acceptance function depends on the geometries of the reflector and receiver. In this paper, we consider only concentrators with rotational symmetry; simplifications resulting from this symmetry are discussed in Section 2.1. In Section 2.2, we analyze a parabolic reflector with a spherical receiver that is placed concentrically around the focal point. The more difficult case of a parabolic reflector with a flat receiver (or equivalently, a cavity receiver with a flat opening) is treated in Section 2.3. In most practical applications, the concentration ratio is sufficiently large (greater than 100) that only small incidence angles need to be considered. The corresponding angles θ are small enough to permit the approximation of $\sin\theta$ by θ. This approximation greatly simplifies the analysis and has been made throughout this paper.

2.1 SYMMETRY CONSIDERATIONS

Figure 2-1 specifies the cylindrical coordinate system used for describing the parabolic dish. The optical axis is along z, and a point P on the dish has the coordinates

$$P = \left(\rho,\alpha,z = \frac{\rho^2}{4}\right) , \tag{2-1}$$

in units where the focal length f is set equal to unity. Consider a ray incident to P, with zenith angle θ and azimuth ϕ, and define a function:

$$f_P(\theta,\phi,\rho,\alpha) = \begin{cases} 1, & \text{if ray reaches receiver;} \\ 0, & \text{if ray does not reach receiver.} \end{cases} \tag{2-2}$$

The angular acceptance function $f(\theta,\phi)$ of the dish is the average of the point acceptance function f_P over the aperture:*

$$f(\theta,\phi) = \frac{1}{\pi b^2} \int_0^b d\rho\ \rho \int_0^{2\pi} d\alpha\ f_P(\theta,\phi,\rho,\alpha) . \tag{2-3}$$

---

*Strictly speaking, a weighting factor $w(\theta,\phi,\rho,\alpha)$ should be included in this integral because uniform illumination of the aperture [as assumed in the definition of $f(\theta,\phi)$] corresponds to nonuniform illumination of the curved reflector surface. Apart from a normalization constant, the weighting factor is the

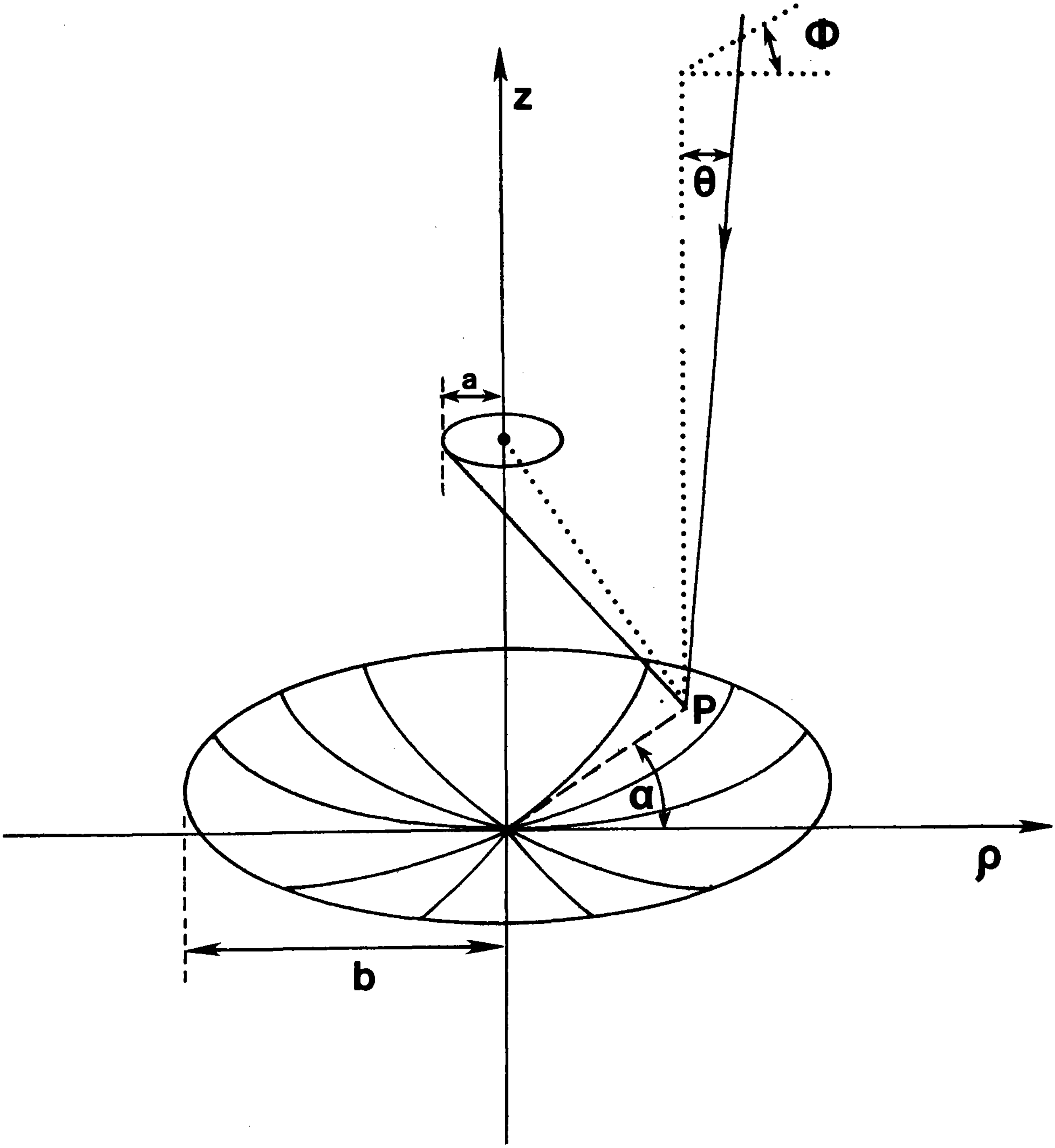

Figure 2-1. Parabolic dish reflector (apex at intersection of ρ and z axes).

Rotational symmetry about the optical axis implies

$$f_P(\theta,\phi,\rho,\alpha) = f_P(\theta,\phi+\gamma,\rho,\alpha+\gamma) \text{ for any } \gamma \quad , \tag{2-4}$$

and in particular for $\gamma = -\alpha$. Letting $\beta = \phi - \alpha$ and noting that the origin of the α integration in Eq. 2-3 is arbitrary, one can transform Eq. 2-3 into the form

$$f(\theta,\phi) = \frac{1}{\pi b^2} \int_0^b d\rho\ \rho \int_0^{2\pi} d\beta\ f_P(\theta,\beta,\rho,0) \quad . \tag{2-5}$$

As expected from azimuthal symmetry, $f(\theta,\phi)$ does not depend on ϕ, i.e.,

$$f(\theta,\phi) = f(\theta) \quad . \tag{2-6}$$

The function f_P was defined with respect to radiation incident on the receiver. However, reversing the direction of the rays does not change the path. Hence, one can treat the receiver as an emitter and ask whether any ray originating from the receiver and reflected at P leaves the aperture in the direction (θ,β). The answer is

$$f_P(\theta,\beta,\rho,\alpha) = \begin{cases} 1, & \text{if yes;} \\ 0, & \text{if no.} \end{cases} \tag{2-7}$$

Because of azimuthal symmetry, it is sufficient to evaluate $f_P(\theta,\beta,\rho,\alpha)$ only on one radius line, $\alpha = 0$, as shown explicitly in Eq. 2-5.

---

product of the reflector surface element and the cosine of the incidence angle on the surface element; it is readily found to be

$$w(\theta,\phi,\rho,\alpha) = 1 + \frac{dz}{d\rho} \sin(\phi - \alpha) \tan\theta \ .$$

The correction term is odd in $\beta = \phi - \alpha$, whereas the point acceptance function f_P is even in β as can be seen from Eqs. 2-9 and 2-10. Therefore, the correction term drops out on integration over β, and $f(\theta)$ is obtained correctly if the weighting factor w is replaced by unity.

2.2 SPHERICAL RECEIVER

The cross section of a parabolic dish with spherical receiver is shown in Fig. 2-2. The focal length is unity and the parabola is given by the equation

$$z = \frac{\rho^2}{4} \quad . \tag{2-8}$$

The geometric concentration ratio, defined as the ratio of aperture area πb^2 over receiver surface area $4\pi a^2$ is

$$C = \frac{b^2}{4a^2} \quad . \tag{2-9}$$

As discussed above, we consider all the rays that originate from the absorber and reflect from some arbitrary point P. These rays fill a cone which can be described as follows: The apex of the cone is at point P and it has rotational symmetry around the line OP because the absorber has rotational symmetry around this line. The edge of the cone is formed by those rays that leave the absorber tangentially and hence the half-angle of the cone is given by

$$\theta_\rho = \arcsin \frac{a}{r} \approx \frac{a}{1 + \frac{\rho^2}{4}} \quad . \tag{2-10}$$

After specular reflection from point P, the rays will form another cone radiating from an apex at P with the same half-angle. The centerline of this cone is the ray that originated from the center of the absorber, O. By assumption, this is also the focal point of the parabola and one of the properties of a parabola is that any ray originating from its focal point will be reflected parallel to the optical axis. Thus the centerline of the reflected cone is along this axis and has $\theta = 0$, and the emerging rays fill the angular region ($\theta < \theta_\rho$, all β). This gives f_P from Eq. 2-7 as

$$f_P\,(\theta,\beta,\rho,0) = \begin{cases} 1, \text{ if } \theta < \theta_\rho; \\ 0, \text{ if } \theta > \theta_\rho. \end{cases} \tag{2-11}$$

This condition does not depend on the azimuth of point P or of the incident ray because a spherical receiver looks the same from all directions. Since θ_ρ decreases with ρ, the minimum of θ_ρ occurs for $\rho = b$ and hence θ_ρ is always greater than or equal to θ_1 defined by

$$\theta_1 = \frac{a}{\left[1 + \left(\frac{b}{2}\right)^2\right]} \quad . \tag{2-12}$$

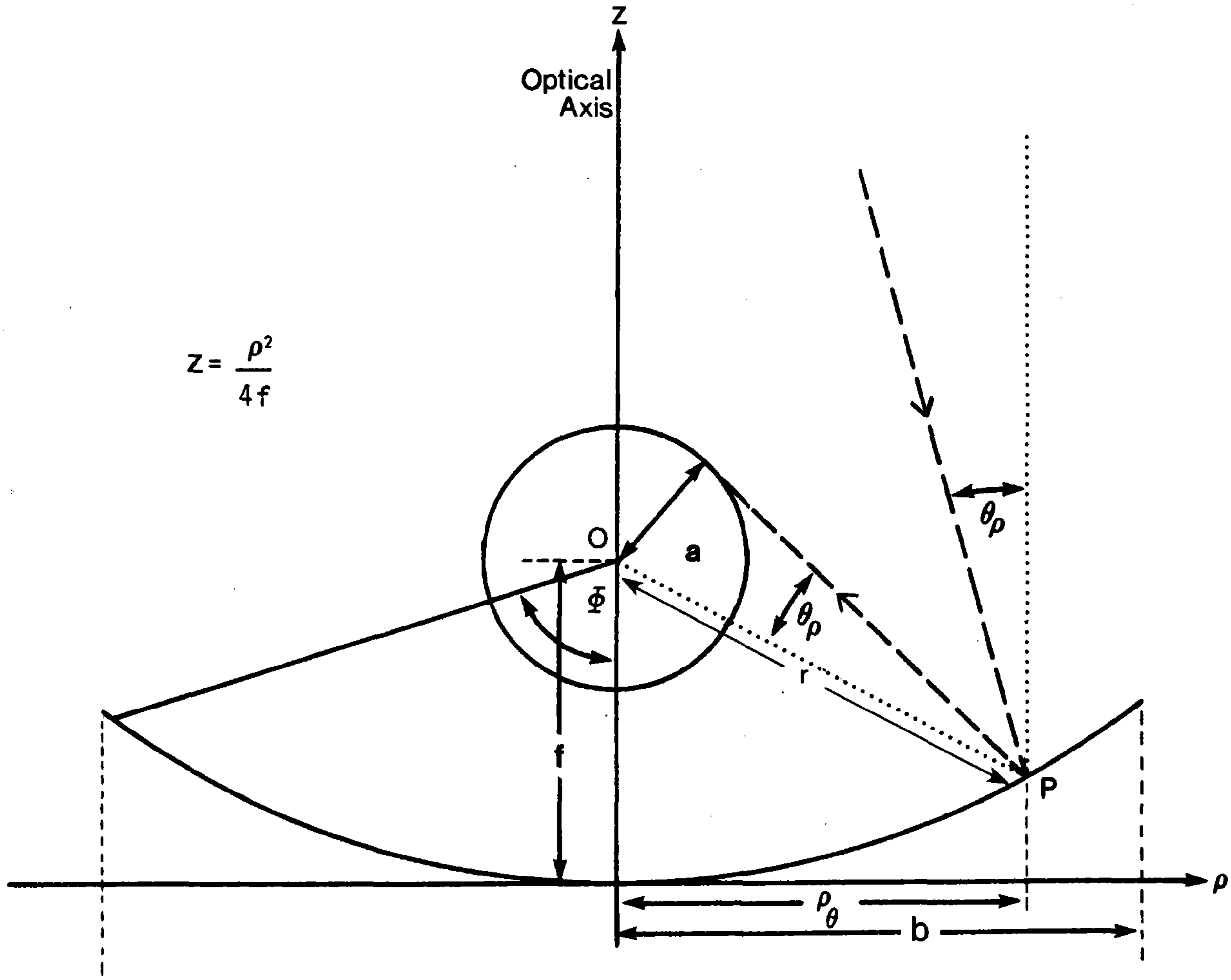

Figure 2-2. Geometrical relations for the calculation of the angular acceptance function of parabolic dish with spherical receiver.
Focal length f is set equal to unity in this paper.

In terms of the concentration ratio C and the rim angle Φ, this angle can be written as

$$\theta_1 = \frac{\sin \Phi}{2\sqrt{C}} \quad . \tag{2-13}$$

Since $\theta_1 < \theta_\rho$, all rays with $\theta < \theta_1$ will satisfy $\theta < \theta_\rho$ and hence all will be received. This implies that $f_{sphere}(\theta)$ equals unity for $\theta < \theta_1$.

Equation 2-4 also shows that θ_ρ reaches its largest value,

$$\theta_2 = a \quad , \tag{2-14}$$

at the apex of the parabola where $\rho = 0$. Since $\theta_2 > \theta_\rho$, all rays with $\theta > \theta_2$ will satisfy $\theta > \theta_\rho$ and hence all will be lost. Because of the assumed high concentration, we can neglect the effect of direct hits on the receiver and $f_{sphere}(\theta)$ becomes zero for $\theta > \theta_2$. (With the assumption of high concentration we also neglect corrections due to the shaded area around the apex of the reflector.)

For angles between θ_1 and θ_2, it is convenient to invert Eq. 2-10 and define

$$\rho_\theta = 2\sqrt{\frac{a}{\theta} - 1} \tag{2-15}$$

as the radius of the point $P = (\rho_\theta, \phi, z)$ where rays with incidence angle θ reach the receiver tangentially. The requirement in Eq. 2-11 for a ray to be received, $\theta < \theta_\rho$, is the same as requiring that $\rho < \rho_\theta$. Thus the active region of the reflector is a circle of radius ρ_θ and area $\pi\rho_\theta^2$. The angular acceptance function is the ratio of this active area to πb^2, the total area, or $f(\theta) = \rho_\theta^2/b^2$. Using the relation

$$\tan \frac{\Phi}{2} = \frac{b}{2} \tag{2-16}$$

to replace a and b by concentration C and rim angle Φ, one can write the final result in the form

$$f_{sphere}(\vec{\theta}) = \begin{cases} 1, \text{ for } \theta < \theta_1; \\ \cot^2 \frac{\Phi}{2} \left[\frac{\tan \Phi/2}{\sqrt{C}\ \theta} - 1 \right], \text{ for } \theta_1 < \theta < \theta_2; \\ 0, \text{ for } \theta > \theta_2; \end{cases} \tag{2-17}$$

with

$$\theta_1 = \frac{\sin \Phi}{2\sqrt{C}} \quad ,$$

and

$$\theta_2 = \frac{\tan \Phi/2}{\sqrt{C}} \quad .$$

Parenthetically we note that Eq. 2-10 is the square of the angular acceptance function of the parabolic trough with cylindrical receiver, as derived in Bendt et al. (1979) (with the replacement $\pi C \rightarrow 2\sqrt{C}$).

For future reference, we point out that the angular acceptance function depends only on the product of $\theta\sqrt{C}$, not on the angle and concentration separately.

2.3 FLAT RECEIVER

The calculation of the angular acceptance function for the flat receiver case is more complicated because, when viewed from a point P on the reflector, the receiver is seen obliquely and appears elliptical.

Rays coming from the receiver toward P form an elliptical cone, both before and after reflection at P. The angular principal axes of this cone are given by

$$\theta_s = \frac{a}{r} \cos \psi \quad \text{and} \quad \theta_\ell = \frac{a}{r} \quad , \tag{2-18}$$

with

$$\cos \psi = \frac{2 - r}{r} \tag{2-19}$$

and

$$r = \sqrt{\rho^2 + (1 - z)^2}$$
$$= 1 + z \quad ,$$

with

$$z = \frac{\rho^2}{4} \quad ;$$

see Fig. 2-3.

After specular reflection, these rays will still form an elliptical cone centered on $\theta = 0$. The equation for the angles θ_e and ϕ_e defining the boundary of this ellipse is

$$\theta_e(\rho, \phi_e) = \frac{\theta_s \theta_\ell}{\sqrt{\theta_s^2 \ \sin^2 \phi_e + \theta_\ell^2 \ \cos^2 \phi_e}} \quad . \tag{2-20}$$

Since the receiver radius, a, is fixed, θ_s and θ_ℓ are functions of ρ only, and θ_e depends only on ρ and ϕ_e.

A ray emitted by the receiver and reflecting at point P will leave the aperture in the direction (θ, β) if and only if (θ, β) lies within the elliptical boundary of Eq. 2-20. Hence, the point acceptance function is

$$f_P(\theta, \beta, \rho, 0) = \begin{cases} 1, \text{ if } \theta < \theta_e \ (\rho, \beta) \text{ of Eq. 2-20} \quad ; \\ 0, \text{ otherwise.} \end{cases} \tag{2-21}$$

All rays with θ less than the minor axis θ_s are within the ellipse; for this case, the azimuthal integration in Eq. 2-5 is trivial with the result

$$\int_0^{2\pi} d\beta \ f_P(\theta, \beta, \rho, 0) = 2\pi, \text{ for } \theta < \theta_s(\rho) \quad . \tag{2-22}$$

Similarly, all of the rays with θ larger than the major axis θ_ℓ are outside the ellipse, and hence

$$\int_0^{2\pi} d\beta \ f_P(\theta, \beta, \rho, 0) = 0, \text{ for } \theta > \theta_\ell \ (\rho) \quad . \tag{2-23}$$

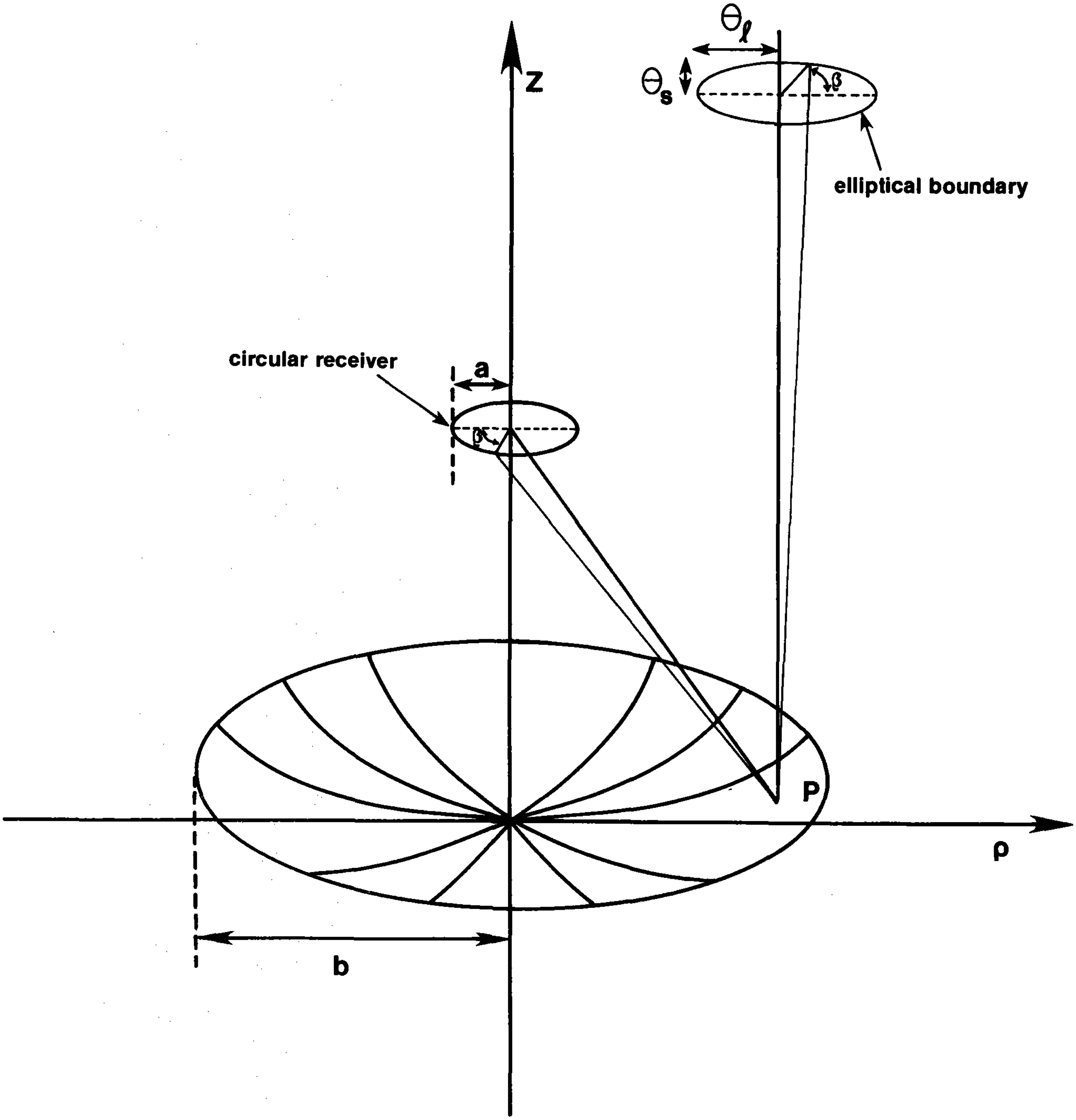

Figure 2-3. Geometrical relations for the calculation of the angular acceptance function of parabolic dish with flat receiver, showing elliptical boundary (Eq. 2-20) of rays emitted by receiver and reflected at P.

For the intermediate case, $\theta_s < \theta < \theta_\ell$, it is convenient to take advantage of reflection symmetry of the ellipse and restrict ϕ to values in the first quadrant, $0 < \beta < \pi/2$, by writing

$$\int_0^{2\pi} d\beta\ f_P(\theta,\beta,\rho,0) = 4\int_0^{\pi/2} d\beta\ f_P(\theta,\beta,\rho,0) \quad . \tag{2-24}$$

To carry out the integration, it is helpful to solve Eq. 2-20 of the elliptical boundary $\theta_e\ (\rho,\beta)$ for β in terms of θ and ρ. Inserting the values of the major and minor axes from Eq. 2-18 and squaring Eq. 2-20, one finds that a ray will be received if it satisifies the inequality:

$$\theta^2 < \theta_e^2(\beta,\rho) = \frac{(a/r)^4 \cos^2 \psi}{(a/r)^2 \cos^2 \psi \sin^2 \beta + (a/r)^2 \cos^2 \beta} \quad . \tag{2-25}$$

This is readily solved for β as a function of θ and ρ,

$$\beta > \arccos\left[\sqrt{(a/r\theta)^2 - 1}\ \cot \psi\right] \equiv \chi(\theta,\rho) \quad . \tag{2-26}$$

Returning to Eq. 2-24, one finds

$$\int_0^{2\pi} d\beta\ f_P(\theta,\beta,\rho,0) = 4\int_{\chi(\theta,\rho)}^{\pi/2} d\beta = 4\left[\frac{\pi}{2} - \chi(\theta,\rho)\right] \quad . \tag{2-27}$$

Inserting Eq. 2-26 and noting that $\frac{\pi}{2}$ - arcos x = arcsin x, one obtains

$$\int_0^{2\pi} d\beta\ f_P(\theta,\beta,\rho,0) = 4 \arcsin\left[\sqrt{(a/r\theta)^2 - 1}\ \cot \psi\right] . \tag{2-28}$$

This completes the integration over the azimuthal variable β in Eq. 2-5. Collecting Eqs. 2-22, 2-23, and 2-28, the intermediate result is

$$f(\theta) = \frac{1}{\pi b^2} \int_0^b d\rho \; \rho \; g(\theta,\rho) \quad , \tag{2-29}$$

with

$$g(\theta,\rho) = \begin{cases} 2\pi, \text{ if } \theta < \theta_s(\rho); \\ 4 \arcsin\left[\sqrt{(a/r\theta)^2 - 1} \; \cot \psi\right], \text{ if } \theta_s(\rho) < \theta < \theta_\ell(\rho); \\ 0, \text{ if } \theta_\ell(\rho) < \theta; \end{cases} \tag{2-30}$$

and

$$\cot \psi = \frac{2 - r}{2\sqrt{r - 1}} \quad . \tag{2-31}$$

There are three regions in θ where f shows different functional behavior. From Eqs. 2-18 and 2-19, θ_s is given by

$$\theta_s = \frac{a(2 - r)}{r^2} \quad , \tag{2-32}$$

and reaches its smallest value when r is at its maximum

$$r_{max} = 1 + \frac{b^2}{4} \quad .$$

In terms of the rim angle Φ, given by

$$\sin \Phi = \frac{b}{1 + \left(b^2/4\right)} \quad , \tag{2-33}$$

the smallest value of θ_s can be written as

$$\theta_1 \equiv \theta_{s,min} = \frac{a}{b} \sin \Phi \cos \Phi \quad . \tag{2-34}$$

For $\theta \leqslant \theta_1$, the function $g(\theta,\rho)$ in Eq. 2-30 equals 2π for all ρ, and the integration is trivial:

$$f(\theta) = 1, \text{ for } \theta \leqslant \theta_1 \quad . \tag{2-35}$$

Similarly, for $\theta \geqslant \theta_2$ (the largest value of θ_ℓ corresponding to $r_{min} = 1$)

$$\theta_2 \equiv \theta_{\ell,\, max} = a = \frac{b}{\sqrt{C}} = \frac{2}{\sqrt{C}} \tan \frac{\Phi}{2} \quad , \tag{2-36}$$

the function $g(\theta,\rho)$ vanishes for all ρ and therefore

$$f(\theta) = 0, \text{ for } \theta \geqslant \theta_2 \quad ; \tag{2-37}$$

C is the geometric concentration ratio $C = \dfrac{b^2}{a^2}$.

For angles between θ_1 and θ_2, the integration is more difficult and must be performed numerically. For computation it is preferable to change the integration variable in Eq. 2-29 from ρ to $r = 1 + \rho^2/4$, and to express the boundaries in Eq. 2-30 in terms of r. The condition

$$\theta \geqslant \theta_\ell(\rho) = \frac{a}{r}$$

can be inverted to

$$r \geqslant \frac{a}{\theta} \equiv r_2 \quad . \tag{2-38}$$

The condition

$$\theta \leqslant \theta_s(\rho) = \frac{a(2 - r)}{r^2}$$

is similarly inverted to

$$r^2 < \frac{a}{\theta}(2 - r) = r_2(2 - r) \quad . \tag{2-39}$$

Solving the quadratic equation and noting that only the positive root is relevant because $r > 1$, one obtains from Eq. 2-39 the bound

$$r < r_1 \equiv -\frac{r_2}{2} + \sqrt{\frac{r_2^2}{4} + 2r_2} \quad . \tag{2-40}$$

Collecting Eqs. 2-29 through 2-40, one can summarize the result for the angular acceptance function $f(\theta)$ of a parabolic dish reflector with a flat receiver as

$$f(\theta) = \begin{cases} 1, \text{ if } \theta < \theta_1 = \dfrac{\sin \Phi \cos \Phi}{\sqrt{C}} \; ; \\ \dfrac{2}{\pi b^2} \displaystyle\int_1^{1+b^2/4} dr\, g(\theta,r), \text{ if } \theta_1 \leq \theta \leq \theta_2 \; ; \\ 0, \text{ if } \theta > \theta_2 = \dfrac{2}{\sqrt{C}} \tan \Phi/2 \; ; \end{cases} \tag{2-41}$$

with

$$g(\theta,r) = \begin{cases} 2\pi, \text{ if } r \leq r_1 = -\dfrac{r_2}{2} + \sqrt{\dfrac{r_2^2}{4} + 2r_2} \; ; \\ 4 \arcsin\left[\dfrac{2 - r}{2\sqrt{r - 1}} \sqrt{\left(\dfrac{b}{r\theta\sqrt{C}}\right)^2 - 1}\,\right], \text{ if } r_1 < r < r_2 \; ; \\ 0, \text{ if } r \geq r_2 = \dfrac{b}{\theta\sqrt{C}} \; ; \end{cases} \tag{2-42}$$

where

$$C = \frac{b^2}{a^2} \tag{2-43}$$

is the geometric concentration ratio. The angular acceptance function depends on only two variables, the rim angle Φ and the combination $\theta\sqrt{C}$. Figure 2-4 shows $f(\theta)$ versus $\theta\sqrt{C}$ for $\Phi = 45°$.

For practical purposes, Eq. 2-41 is rather tedious, but sufficient accuracy is maintained if the angular acceptance function in the intermediate region is approximated by a polynomial expansion in the variable $\theta\sqrt{C}$;

$$f(\theta) \approx \begin{cases} 1, \text{ for } \theta < \tilde{\theta}_1 \approx \theta_1 = \dfrac{\sin\Phi\cos\Phi}{\sqrt{C}} \; ; \\[2ex] a + b\,(C\theta^2) + c\,(C\theta^2)^2 + \ldots, \text{ for } \tilde{\theta}_1 < \theta < \tilde{\theta}_2 \; ; \\[2ex] 0, \text{ for } \theta > \tilde{\theta}_2 \approx \theta_2 = \dfrac{2}{\sqrt{C}} \tan\dfrac{\Phi}{2} \; . \end{cases} \tag{2-44}$$

The coefficients, a, b, c, ..., depend on the rim angle Φ and are listed in Table 2-1. They were obtained by minimizing the difference in the areas under the curve, $\int d\theta\, f(\theta)$, between the exact angular acceptance function and the polynomial fit. The angles $\tilde{\theta}_1$ and $\tilde{\theta}_2$, listed in Table 2-1 as $v_1 = \tilde{\theta}_1\sqrt{C}$ and $v_2 = \tilde{\theta}_2\sqrt{C}$, are the angles where the polynomial fit takes on the values 1 and 0, respectively. Two sets of coefficients are given in Table 2-1, depending on the accuracy desired. Table 2-1a provides a three-term expansion, for rim angles from $\Phi = 30°$ to $\Phi = 60°$, in 5° increments. Table 2-1b gives the coefficients for the four-term expansion with 1° increments in Φ. The values for other rim angles can be determined by interpolation. Within the accuracy of Fig. 2-4, the three-term polynomial expansion is almost indistinguishable from the exact results.

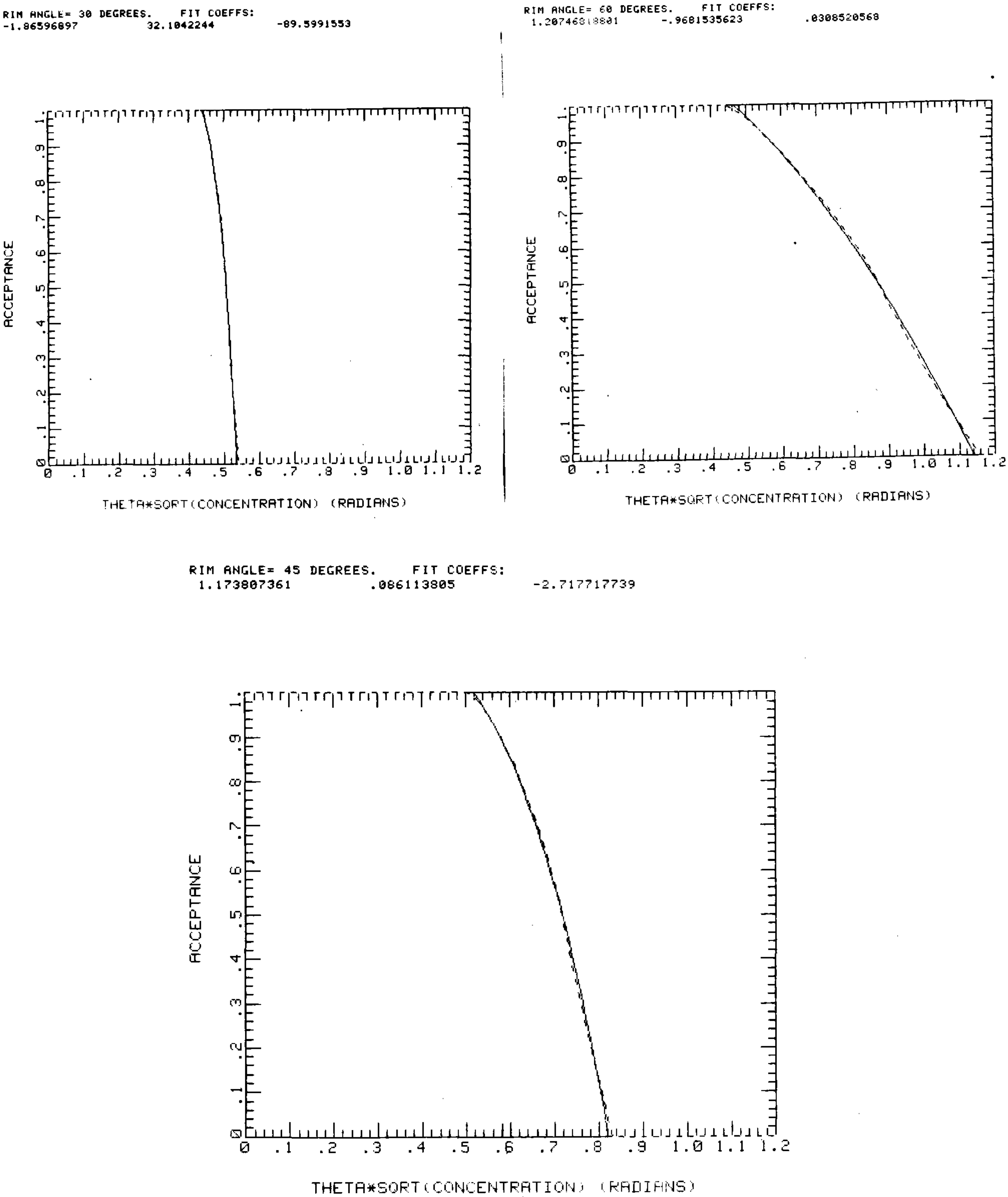

Figure 2-4. Angular acceptance function for parabolic dish with flat receiver.

Solid line: exact result; dashed line: polynomial approximation with three terms.

Table 2-1. COEFFICIENTS OF POLYNOMIAL FIT EQ. 2-44 TO ANGULAR ACCEPTANCE FUNCTION, WITH $v_1 = \tilde{\theta}_1 \sqrt{C}$ and $v_2 = \tilde{\theta}_2 \sqrt{C}$; (a) THREE-TERM EXPANSION, AND (b) FOUR-TERM EXPANSION

(a)

Φ [degrees]	a	b	c	v_1	v_2
30	-1.8660	32.1042	-89.5992	0.4355	0.5342
35	0.2309	8.7987	-23.7599	0.4785	0.6284
40	0.8866	2.4950	-8.0311	0.5053	0.7226
45	1.1738	0.0861	-2.7177	0.5189	0.8205
50	1.2646	-0.7577	-0.8522	0.5179	0.9231
55	1.2466	-0.9444	-0.2199	0.4969	1.0290
60	1.2075	-0.9682	0.0309	0.4645	1.1407

(b)

Φ [degrees]	a	b	c	d	v_1	v_2
30	-4.4647	65.5256	-231.6741	199.6752	0.4365	0.534
31	-4.5916	65.3298	-230.3732	215.6702	0.4806	0.553
32	-3.2651	48.6801	-165.7419	145.2926	0.4536	0.572
33	-2.9694	43.7084	-144.6810	125.8221	0.4517	0.591
34	-2.6752	39.2132	-126.3405	108.4094	0.4598	0.610
35	-1.8817	30.1432	-94.2664	76.2152	0.4682	0.629
36	-0.9984	20.3357	-60.3045	41.6597	0.4708	0.647
37	-0.8803	18.5920	-54.0918	37.6157	0.4498	0.666
38	-0.5546	15.3131	-44.0733	29.8485	0.4757	0.686
39	-0.2971	12.7096	-36.1594	23.7696	0.4879	0.705
40	-0.1744	11.2891	-31.6287	20.5410	0.4758	0.725
41	0.0281	9.3233	-25.9283	16.2998	0.4729	0.745
42	0.2034	7.7235	-21.4737	13.1345	0.4948	0.765
43	0.3484	6.4039	-17.8527	10.6252	0.4993	0.785
44	0.4679	5.3146	-14.9032	8.6317	0.4999	0.805
45	0.5406	4.5794	-12.8446	7.2859	0.4916	0.826
46	0.6616	3.6087	-10.4495	5.7546	0.5010	0.846
47	0.7394	2.9432	-8.7703	4.7180	0.5013	0.867
48	0.7824	2.5347	-7.7098	4.1138	0.4972	0.889
49	0.8420	2.0125	-6.4216	3.3377	0.4924	0.910
50	0.8969	1.5651	-5.3625	2.7276	0.4924	0.931
51	0.9437	1.1781	-4.4598	2.2215	0.4904	0.952
52	0.9788	0.8666	-3.7263	1.8195	0.4852	0.974
53	1.0122	0.5920	-3.1055	1.4926	0.4834	0.996
54	1.0388	0.3587	-2.5779	1.2208	0.4793	1.018
55	1.0557	0.1827	-2.1673	1.0151	0.4721	1.041
56	1.0762	0.0037	-1.7782	0.8258	0.4686	1.063
57	1.0897	-0.1388	-1.4587	0.6730	0.4622	1.086
58	1.1025	-0.2654	-1.1845	0.5464	0.4575	1.109
59	1.1123	-0.3772	-0.9430	0.4376	0.4514	1.132
60	1.1166	-0.4623	-0.7488	0.3516	0.4425	1.156

SECTION 3.0

CALCULATION OF FLUX AT RECEIVER

3.1 EFFECTIVE SOURCE

In a real concentrator, rays are incident from a range of directions and are reflected by an imperfect reflector surface which causes further angular dispersion. From the point of view of the receiver, it does not matter whether the angular deviation of a ray from the design direction originates at the radiation source or at the reflector. This is illustrated in Fig. 3-1. In Fig. 3-1a, a ray from a point source S strikes the reflector at a point R and would reach a point Q of the receiver if the reflector were perfect. A real reflector differs from the design slope by an error $\vec{\theta}_{slope}$, and thus the reflected ray reaches the receiver at Q', an angle $2\vec{\theta}_{slope}$ away from Q. The same reflected ray would have resulted from a perfect reflector if the incident ray had come from S', an angle $2\vec{\theta}_{slope}$ away from the point source S, as shown in Fig. 3-1b. In general, the distribution of slope errors is nearly gaussian, and the corresponding flux distribution at the receiver is indicated by the curves in Figs. 3-1a and b.

In three-dimensional space, two angular variables are required to specify any direction. Henceforth, we specify all angles as two-dimensional vectors $\vec{\theta} = (\theta_x, \theta_y)$, with x and y components θ_x and θ_y measured from the optical axis of the parabolic reflector. In most practical cases, the distribution functions for brightness and optical errors have rotational symmetry and depend only on $\theta = |\vec{\theta}|$; nonetheless, it is helpful to write the convolution integrals in two-dimensional notation.

There may be several independent sources of optical errors in a real concentrator: lack of perfect specularity (Pettit 1977), macroscopic surface deviations in position and slope, displacement of the receiver, tracking errors, etc. Each of these errors can be characterized by a probability density function: $E_{specular}(\vec{\theta})$, $E_{contour}(\vec{\theta})$, $E_{displacement}(\vec{\theta})$, $E_{tracking}(\vec{\theta})$, etc; for each type of error, the corresponding $E(\vec{\theta})\, d^2\theta$ is the probability that a ray is scattered into an angular interval $d^2\theta$ around an angle $\vec{\theta}$ (measured from the design direction). The effect of all these errors can be combined into a single effective error distribution $E_{optical}(\vec{\theta})$ which is the convolution of the individual functions. For example, if lack of specularity, contour deviations, and receiver displacements are the only relevant errors, the effective distribution is

$$E_{optical}(\vec{\theta}) = \iint d^2\,\theta_1\, E_{specular}(\vec{\theta} - \vec{\theta}_1) \iint d^2\,\theta_2\, E_{contour}[(\vec{\theta}_1 - \vec{\theta}_2)/2]$$

$$E_{displacement}(\vec{\theta}_2) \quad . \tag{3-1}$$

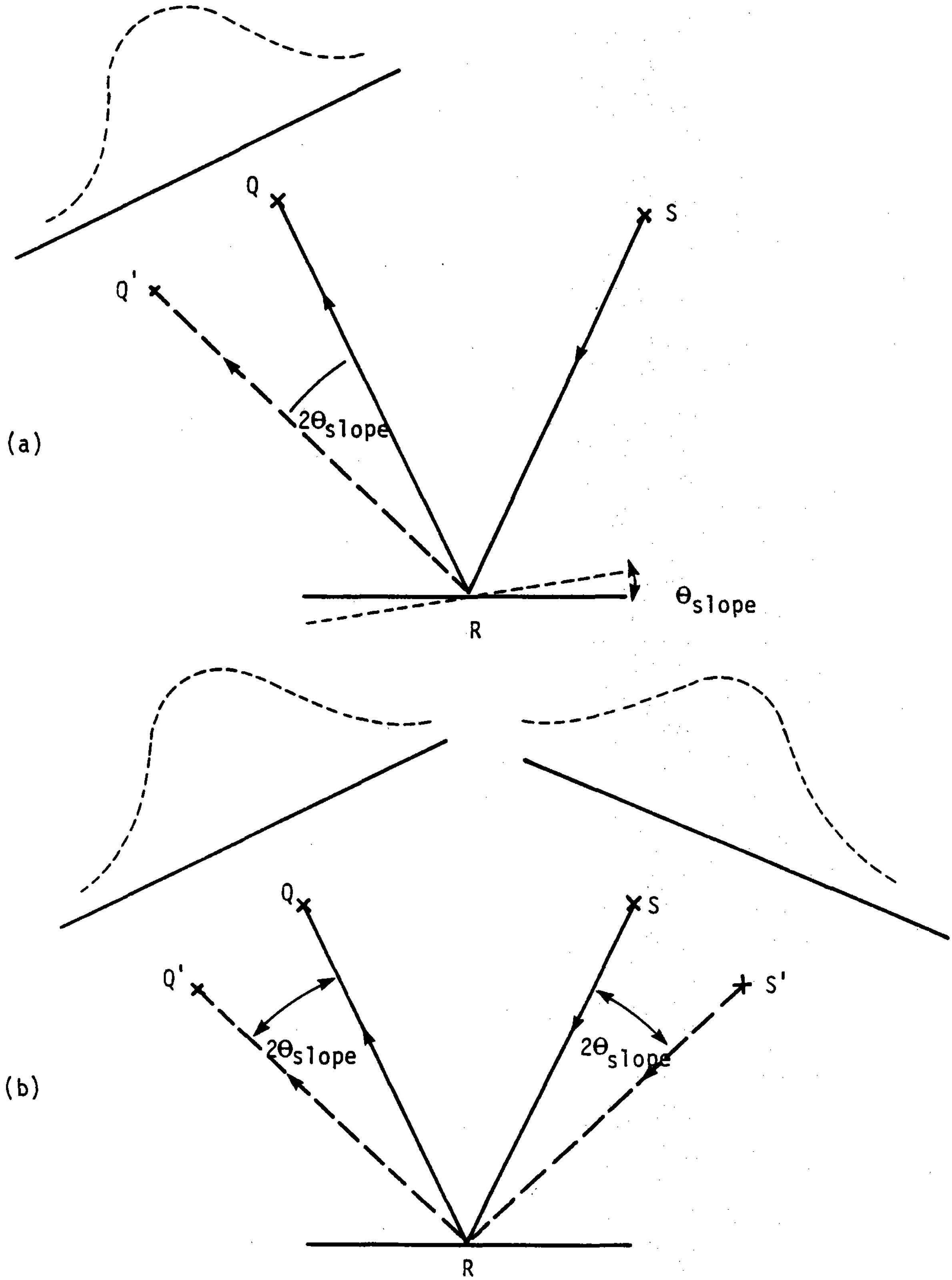

Figure 3-1. Equivalence between (a) imperfect reflector with point source and (b) perfect reflector with smeared source.

The factor of 1/2 in $E_{contour}$ $[(\vec{\theta}_1 - \vec{\theta}_2)/2]$ results from Snell's law of reflection.

The angular distribution of radiation from a real source like the sun is given by a distribution B_{source} $(\vec{\theta}_{in})$, the brightness given in W/m^2 sterad for radiation incident from the direction $\vec{\theta}_{in}$. If the mirror errors are characterized by a probability density function $E_{optical}(\vec{\theta})$, then the reflected intensity in the direction $\vec{\theta}$ (measured from the design direction) is

$$d^2B(\vec{\theta}, \vec{\theta}_{in}) = E_{optical}(\vec{\theta} - \vec{\theta}_{in})\, B_{source}(\vec{\theta}_{in})\, d^2\theta_{in} \quad , \tag{3-2}$$

where $(\vec{\theta} - \vec{\theta}_{in})$ is the optical error and $B_{source}(\vec{\theta}_{in})\ d^2\theta_{in}$ is the intensity of radiation coming from an angular region of width $d^2\theta_{in}$ around $\vec{\theta}_{in}$. Integrating over $d^2\theta_{in}$, one obtains the equivalent effective source

$$B_{eff}(\vec{\theta}) = \iint E_{optical}(\vec{\theta} - \vec{\theta}_{in})\, B_{source}(\vec{\theta}_{in})\, d^2\theta_{in} \quad . \tag{3-3}$$

The limits of integration can be extended to infinity because in practice all the distributions will be negligible outside a range of a few degrees.

In most cases, the optical errors can be assumed to be approximately gaussian. This is the most reasonable assumption; it is supported by the limited data that are available (Butler and Pettit 1977). Even if the distributions for individual optical errors are not quite gaussian, the central limit theorem of statistics (Cramer 1947) implies that the distribution resulting from their convolution can be expected to be nearly gaussian, at least as long as the distribution is not dominated by a single nongaussian component.

Since the convolution of two gaussians with zero mean and standard deviations σ_1 and σ_2 is again a gaussian distribution, with standard deviation given by $\sigma^2 = \sigma_1^2 + \sigma_2^2$, it is reasonable to approximate the effective optical error distribution $E_{optical}$ $(\vec{\theta})$ by a gaussian of variance $\sigma^2_{optical}$, the latter being, of course, the quadratic sum of all the widths of the individual error contributions.

$$\sigma^2_{optical} = \sigma^2_{specular} + (2\sigma_{contour})^2 + \sigma^2_{displacement} + \cdots \tag{3-4}$$

In that case, the effective source is given by

$$B_{eff}(\vec{\theta}) = \frac{1}{2\pi\sigma_{optical,x}\,\sigma_{optical,y}} \int_{-\infty}^{\infty} d^2\theta' \exp\left[-\frac{\theta_x^2}{2\sigma^2_{optical,x}} - \frac{\theta_y^2}{2\sigma^2_{optical,y}}\right] B_{source}(\vec{\theta} - \vec{\theta}') \quad . \tag{3-5}$$

We have indicated different standard deviations in different orthogonal directions x and y to allow for the possibility of error distributions without rotational symmetry. The orthogonal directions need not be x and y; in fact, a more realistic case is a distribution with different widths in azimuthal and radial directions. In any case, Eq. 3-4 is to be used for each of the two orthogonal directions separately.

Before closing this subsection, we point out that replacing contour errors by an effective source involves a slight approximation, and that Fig 3.1 is misleading with regard to the situation in three dimensions. At oblique angles of incidence ψ, a circular gaussian distribution of contour errors with width σ results in an elliptic gaussian distribution of the reflected rays, with width σ in the plane spanned by the reflected ray and by the surface normal and with width $\sigma \cos \psi$ in the plane perpendicular to it, as shown by Biggs and Vittoe. The use of an effective source assumes that the distribution of the reflected rays remains a circular gaussian for all points on the reflector. This is exact at the apex of the parabola, where the incidence angle vanishes. At the rim of the parabola, the incidence angle reaches its maximum $\psi = \Phi/2$, where Φ is the rim angle. In most practical applications (certainly in solar energy), the rim angle will be less than 60°; hence the factor $\cos \psi$ will be close to unity when averaged over the aperture, and the effective source is an excellent approximation. This is necessary in order to permit calculation of intercepted radiation by a formula as simple as Eq. 3-6. The approximation is conservative; i.e., it underpredicts the intercepted radiation.

3.2 FLUX AT RECEIVER

The effective source function $B_{eff}(\vec{\theta})$ of Eq. 3-3 gives the intensity of radiation (W/m^2 sterad) coming from the direction $\vec{\theta}$; it accounts correctly for the shape of the source and for all optical errors. The angular acceptance function $f(|\vec{\theta}|)$ states how much of this radiation is transmitted to the receiver.* The total flux intercepted by the receiver is obtained by multiplying these two functions together and integrating over all incidence angles,

$$I_{in} = \iint_{-\infty}^{\infty} d^2\theta \; f(|\vec{\theta}|) \; B_{eff} \, (\vec{\theta}) \quad . \tag{3-6}$$

The receiver size enters through the concentration ratio C in the angular acceptance function. The derivative of I_{in} with respect to C yields the spatial flux distribution at the receiver. The distribution of incidence angles can be obtained, to a good approximation, from the derivative of I_{in} with respect to the rim angle.

The formulation is equivalent to a detailed computer ray-trace program. It is much simpler and faster, requiring at most a double integration. (Unless one of the optical errors is nongaussian and dominates, in which case a further integration is needed to convolute the optical errors correctly.) The relevant parameters and their interrelation are clearly identified.

3.3 RMS WIDTH FOR 2-D DISTRIBUTIONS

The widths σ_x and σ_y (dropping the subscript "optical") appearing in the Gaussian error distribution in Eq. 3-5 are rms angular widths measured along the x and y directions:

$$\begin{aligned}
\langle\theta_x^2\rangle &= \int d^2\,\theta\;\theta_x^2 \quad E\left(\theta_x,\,\theta_y\right) \\
&= \int_{-\infty}^{\infty} d\,\theta_x\;\theta_x^2 \int_{-\infty}^{\infty} d\,\theta_y\;\frac{1}{2\pi\sigma_x\sigma_y}\;\exp\left[-\frac{\theta_x^2}{2\sigma_x^2}-\frac{\theta_y^2}{2\sigma_y^2}\right] \\
&= \int_{-\infty}^{\infty} d\,\theta_x\;\theta_x^2\;\frac{1}{\sqrt{2\pi}\,\sigma_x}\;\exp\left[-\frac{\theta_x^2}{2\sigma_x^2}\right] \\
&= \sigma_x^2 \quad .
\end{aligned} \tag{3-7}$$

*$f(\vec{\theta})$ is defined as a purely geometrical quantity. Absorption losses are accounted for by a multiplicative factor.

The rms width averaged over azimuthal directions is

$$\langle \vec{\theta}^2 \rangle = \langle \theta_x^2 + \theta_y^2 \rangle$$

$$= \sigma_x^2 + \sigma_y^2 \quad . \tag{3-8}$$

In case of azimuthal symmetry, the widths σ_x and σ_y are equal,

$$\sigma_x = \sigma_y = \sigma \quad , \tag{3-9}$$

and the elliptic gaussian becomes a circular gaussian

$$E(\theta) = \frac{1}{2\pi\sigma^2} \exp\left[-\frac{\theta^2}{2\sigma^2}\right] . \tag{3-10}$$

The associated rms width is $\sqrt{2}$ times σ

$$\sqrt{\langle \theta^2 \rangle} = \sqrt{2}\,\sigma \quad . \tag{3-11}$$

SECTION 4.0

EXAMPLE: CIRCULAR GAUSSIAN SOURCE

Great simplification results if the effective source is circular gaussian. This is obviously the case if both source and optical errors are circular gaussian. It is also a good approximation if any nongaussian distributions have a narrow width compared to gaussian distributions. For example, the width of the sun is

$$\sigma_{sun} = 2.6 \text{ mrad} \tag{4-1}$$

under clear sky conditions.* Even though the brightness of the solar disk is not a gaussian distribution, one can treat the effective source as gaussian with rms width σ given by

$$\sigma^2 = \sigma^2_{optical} + \sigma^2_{sun} , \tag{4-2}$$

whenever the gaussian optical errors are sufficiently large. As shown in Biggs and Vittoe, the error in the intercepted radiation resulting from such a gaussian approximation is less than 1% if $\sigma_{optical} > 10$ mrad.

It is convenient to define a dimensionless intercept factor,

$$\gamma = \frac{I_{in}}{\iint d^2\theta \; B(\vec{\theta})} , \tag{4-3}$$

as the fraction of the incident flux $\iint d^2\theta \; B(\vec{\theta})$ which is intecepted by the receiver. With the gaussian approximation for the effective source, the intercept factor takes the form

$$\gamma_{gauss} = \frac{1}{\sigma^2} \int_0^\infty d\theta \; \theta \; f(\theta) \exp\left[-\frac{\theta^2}{2\sigma^2}\right] , \tag{4-4}$$

---

*The exact value depends on the amount of circumsolar radiation, see SERI/TR-34-093 (Bendt and Rabl 1979a).

assuming rotational symmetry. Since $f(\theta)$ is really a function of the product $\sqrt{C}\ \theta$, γ_{gauss} depends only on $\sigma\sqrt{C}$ and on rim angle Φ. When $f(\theta)$ is approximated by the polynomial expansion Eq. 2-44, the integration can be carried out in closed form to yield

$$\begin{aligned}\gamma_{gauss}(z) = 1 &- \exp\left(-\frac{v_1^2}{2z}\right) \\ &+ \exp\left(-\frac{v_1^2}{2z}\right)\left[a + b\left(v_1^2 + 2z\right) + c\left(v_1^4 + 4zv_1^2 + 8z^2\right)\right. \\ &\left.+ d\left(v_1^6 + 6zv_1^4 + 24z^2v_1^2 + 48z^3\right)\right] \\ &- \exp\left(-\frac{v_2^2}{2z}\right)\left[a + b\left(v_2^2 + 2z\right) + c\left(v_2^4 + 4zv_2^2 + 8z^2\right)\right. \\ &\left.+ d\left(v_2^6 + 6zv_2^4 + 24z^2v_2^2 + 48z^3\right)\right],\end{aligned} \tag{4-5}$$

with

$$z = \sigma^2 C,$$

and the coefficients a, b, c, d, v_1, and v_2 given in Table 2-1. This function is plotted in Fig. 4-1 for several values of Φ.

To demonstrate how the intercept factor is to be used, we recall that γ is defined as a purely geometrical quantity. Absorption losses are treated by means of a multiplicative factor. For example, if

I_b = incident flux on aperature of parabolic reflector (in W/m^2),
A = aperture area of reflector,
ρ = reflectance of reflector, and
α = absorptance of receiver,

then the power absorbed by the receiver (in W) is

$$\text{power} = \rho\ \alpha\ \gamma\ A\ I_b\ . \tag{4-6}$$

Let us assume a parabolic dish with rim angle $\Phi = 45°$ and a flat one-sided receiver with geometric concentration ratio $C = 1000$ (i.e., the ratio of aperture over receiver diameter is $\sqrt{1000} = 31.6..$). With an optical error $\sigma_{optical} = 10$ mrad, the beam width is

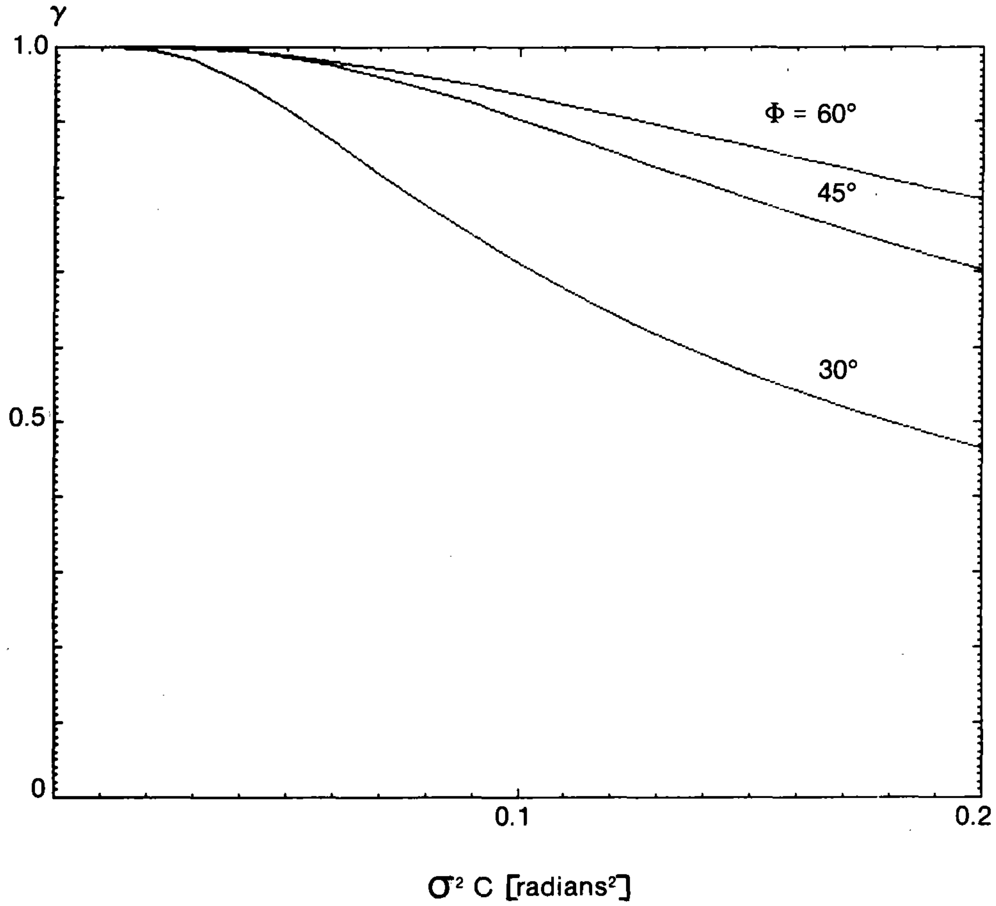

Figure 4-1. Intercept factor γ for parabolic dish with flat receiver, geometric concentration C, and rim angle Φ, if source is gaussian with width σ.

$$\sigma = \sqrt{10^2 + 2.6^2} \text{ mrad} = 10.33.. \text{ mrad} \quad .$$

From Fig. 4-1, we read off an intercept factor of $\gamma = 0.89$ corresponding to the abscissa $z = \sigma^2 C = 0.107$. On a clear day, the direct (or beam) insolation is approximately

$$I_b = 1000 \quad W/m^2 \; .$$

With $\rho = 0.9$, $\alpha = 0.95$, and an aperture area of 10 m^2, this yields the power absorbed by the receiver as

$$\begin{aligned} \text{power} &= \rho\alpha\gamma A I_b \\ &= 0.9 \times 0.95 \times 0.89 \times 10 \text{ m}^2 \times 1000 \text{ W/m}^2 \\ &= 7610 \text{ W} \quad . \end{aligned}$$

For further applications and for numerical examples, the reader is referred to the papers by Bendt et al.

SECTION 5.0

REFERENCES

1. Bendt, P. and Rabl, A. 1979a. "Effect of Circumsolar Radiation on Performance of Focusing Solar Collectors." Golden, CO: Solar Energy Research Institute; SERI/TR-34-093.

2. Bendt, P. and Rabl, A. 1979b. "Optimization of Concentration Ratio of Parabolic Dish Solar Collectors." Golden, CO: Solar Energy Research Institute; SERI/TR-34-257.

3. Bendt, P.; Rabl, A.; Gaul, H. W. and Reed, K. A. 1979. "Optical Analysis and Optimization of Line Focus Solar Collectors." Golden, CO: Solar Energy Research Institute; SERI/TR-34-092. September.

4. Biggs, F. and Vittoe, E. N. "The Helios Model for the Optical Behavior of Reflecting Solar Concentrators." Sandia Laboratories Report; SAND 76-0347.

5. Butler, B. L. and Pettit, R. B. 1977. "Optical Evaluation Techniques for Reflecting Solar Concentrators." Optics Applied to Solar Energy Conversion. SPIE Vol. 114, p. 43.

6. Cramer, H. 1947. "Mathematical Methods of Statistics." Princeton, NJ; Princeton University Press.

7. Harper, D. A.; Hildebrand, R.; Stiening, R. and Winston, R. 1976. Applied Optics. Vol 15, p. 53.

8. O'Neill, M. J. and Hudson, S. L. 1978. "Optical Analysis of Paraboloidal Solar Concentrators." Proceedings 1978 Annual Meeting, U.S. Section of Int. Solar Energy Soc. August 1978; Denver, CO. Vol 2.1: p. 855.

9. Pettit, R. B. 1977. "Characterization of the Reflected Beam Profile of Solar Mirror Materials." Solar Energy. Vol 19, p. 733.

10. Rabl, A. 1976. "Comparison of Solar Concentrators." Solar Energy. Vol. 18, p. 93.

11. Schrenk, G. M. 1963. "Analysis of Solar Reflectors-Mathematical Theory and Methodology for Simulation of Real Reflectors." GMC-AO-EDR3693.

12. Treadwell, G. W. 1976. "Design Considerations for Parabolic Cylindrical Solar Collectors." Sandia Laboratories Report; SAND 76-0082.

13. Wen, L.; Huang, L.; Poon, P. and Carley, W. 1979. "Comparative Study of Solar Optics for Parabolidal Concentrators." American Society of Mechanical Engineers. Paper 79-WA/Sol-8. December.

Document Control Page	1. SERI Report No. TR-631-336	2. NTIS Accession No.	3. Recipient's Accession No.

4. Title and Subtitle Optical Analysis of Point Focus Parabolic Radiation Concentrators	5. Publication Date April 1980 6.
7. Author(s) P. Bendt; A. Rabl	8. Performing Organization Rept. No.
9. Performing Organization Name and Address Solar Energy Research Institute 1617 Cole Blvd. Golden, CO 80401	10. Project/Task/Work Unit No. Task No. 3527 11. Contract (C) or Grant (G) No. (C) (G)
12. Sponsoring Organization Name and Address	13. Type of Report & Period Covered Technical Report 14.

15. Supplementary Notes

16. Abstract (Limit: 200 words)

A simple formalism is developed for analyzing the optical performance of point focus parabolic radiation concentrators. To account for off-axis aberrations of the parabola, an angular acceptance function is defined as that fraction of a beam of parallel radiation incident on the aperture which would reach the receiver if the optics were perfect. The radiation intercepted by the receiver of a real concentrator is obtained as convolution of angular acceptance function, of optical error distribution, and of angular brightness distribution of the radiation source. Losses resulting from absorption in the reflector as reflection at the receiver is treated by a multiplicative factor $\rho\alpha$ where ρ = reflectance of the reflector and α = absorptance of the receiver. For numerical calculations, this method is far more accurate and timesaving than the ray-tracing method. In many cases, these are approximations whereby the results can be obtained by reading a graph or evaluating a simple curve fit.

17. Document Analysis

a. Descriptors Point Focus Solar Collectors; Optical Efficiency; Performance; Performance Testing; Radiation Flux; Gaussian Processes

b. Identifiers/Open-Ended Terms

c. UC Categories UC-62

18. Availability Statement NTIS U. S. Dept. of Commerce 5285 Port Royal Rd. Springfield, VA 22161	19. No. of Pages 39 20. Price $4.50

Form No. 8200-13 (6-79)

☆ U.S. GOVERNMENT PRINTING OFFICE: 1980 - 677-175 REGION NO. 8